

Diffraction optical elements utilized for efficiency enhancement of photovoltaic modules

1-1-2011

I. Mingareev

University of Central Florida

R. Berlich

University of Central Florida

T. J. Eichelkraut

University of Central Florida

H. Herfurth

S. Heinemann

See next page for additional authors

Find similar works at: <https://stars.library.ucf.edu/facultybib2010>

University of Central Florida Libraries <http://library.ucf.edu>

Recommended Citation

Mingareev, I.; Berlich, R.; Eichelkraut, T. J.; Herfurth, H.; Heinemann, S.; and Richardson, M. C., "Diffraction optical elements utilized for efficiency enhancement of photovoltaic modules" (2011). *Faculty Bibliography 2010s*. 1672.

<https://stars.library.ucf.edu/facultybib2010/1672>

This Article is brought to you for free and open access by the Faculty Bibliography at STARS. It has been accepted for inclusion in Faculty Bibliography 2010s by an authorized administrator of STARS. For more information, please contact lee.dotson@ucf.edu.

Authors

I. Mingareev, R. Berlich, T. J. Eichelkraut, H. Herfurth, S. Heinemann, and M. C. Richardson

Diffraction optical elements utilized for efficiency enhancement of photovoltaic modules

I. Mingareev,^{1,*} R. Berlich,^{1,2} T. J. Eichelkraut,^{1,2} H. Herfurth,³
S. Heinemann,³ and M. C. Richardson¹

¹Townes Laser Institute, University of Central Florida, 4000 Central Florida Blvd., Orlando, Florida 32816, USA

²Department of Physics and Astronomy, Friedrich Schiller University of Jena, Max-Wien-Platz 1, 07743 Jena, Germany

³Fraunhofer Center for Laser Technology, 46025 Port Street, Plymouth, Michigan 48170, USA

*mingareev@ucf.edu

<http://www.townes.ucf.edu>

Abstract: Common solar cells used in photovoltaic modules feature metallic contacts which partially block the sunlight from reaching the semiconductor layer and reduce the overall efficiency of the modules. Diffraction optical elements were generated in the bulk glass of a photovoltaic module by ultrafast laser irradiation to direct light away from the contacts. Calculations of the planar electromagnetic wave diffraction and propagation were performed using the rigorous coupled wave analysis technique providing quantitative estimations for the potential efficiency enhancement of photovoltaic modules.

© 2011 Optical Society of America

OCIS codes: (050.1970) Diffraction optics; (050.7330) Volume gratings; (140.3390) Laser materials processing; (140.7090) Ultrafast lasers; (350.6050) Solar energy.

References and links

1. S. R. Wenham, M. A. Green, M. E. Watt and R. Corkish, *Applied Photovoltaics*, 2nd ed. (Earthscan Publications Ltd., 2007).
2. L. Wen, L. Yueqiang, C. Jianjun, C. Yanling, W. Xiaodong, and Y. Fuhua, "Optimization of grid design for solar cells," *J. Semicond.* **31**(1), 014006 (2010).
3. P. Benítez, J. C. Miñano, P. Zamora, R. Mohedano, A. Cvetkovic, M. Buljan, J. Chaves, and M. Hernández, "High performance Fresnel-based photovoltaic concentrator," *Opt. Express* **18**(S1), A25–A40 (2010).
4. J. E. Cotter, R. B. Hall, M. G. Mauk, and A. M. Barnett, "Light trapping in silicon-film solar cells with rear pigmented dielectric reflectors," *Prog. Photovoltaics* **7**, 261–274 (1999).
5. J. Jaus, H. Pantsar, J. Eckert, M. Duell, H. Herfurth, and D. Doble, "Light management for reduction of bus bar and gridline shadowing in photovoltaic modules," in *Proceedings of the IEEE Photovoltaic Specialists Conference (IEEE 2010)*, pp. 979–983 (2010).
6. S. Sinzinger and J. Jahns, "Integrated micro-optical imaging system with a high interconnection capacity fabricated in planar optics," *Appl. Opt.* **36**, 4729–4735 (1997).
7. Y. Kuroiwa, N. Takeshima, Y. Narita, S. Tanaka, and K. Hirao, "Arbitrary micropatterning method in femtosecond laser microprocessing using diffraction optical elements," *Appl. Phys. Lett.* **12**, 1908–1915 (2004).
8. K. M. Davis, K. Miura, N. Sugimoto, and K. Hirao, "Writing waveguides in glass with a femtosecond laser," *Opt. Lett.* **21**, 1729–1731 (1996).
9. M. G. Moharam, E. B. Grann, D. A. Pommet, and T. K. Gaylord, "Formulation for stable and efficient implementation of the rigorous coupled-wave analysis of binary gratings," *J. Opt. Soc. Am. A* **12**, 1068–1076 (1995).
10. J. Choi, M. Ramme, T. Anderson, and M. C. Richardson, "Femtosecond laser written embedded diffraction optical elements and their applications," *Proc. SPIE* **7589**, 75891A (2010).

11. R. W. Gerchberg and W. O. Saxton, "A practical algorithm for the determination of phase from image and diffraction plane pictures," *Optik (Stuttgart)* **35**, 237–246 (1972).
 12. P. Russbueldt, T. Mans, J. Weitenberg, H. D. Hoffmann and R. Poprawe, "Compact diode-pumped 1.1 kW Yb:YAG Innoslab femtosecond amplifier," *Opt. Lett.* **35**(24), 4169–4171 (2010).
-

1. Introduction

The most commonly used technology in the photovoltaic industry relies on crystalline silicon (c-Si) modules. Usually for the collection of the photocurrent highly conductive metals such as aluminum or silver are deposited on the front and the backside of the solar cell. As some portion of the active semiconductor area is covered by the metal deposited on the front, the solar radiation is partially blocked from reaching the silicon surface. Thus the area covered by the metalization needs to be kept to a minimum in order to reduce shadowing energy losses. The metallic contacts are usually deposited in a periodical pattern of relatively narrow grid fingers connected by much wider bus bars. The spacing and the width of grid fingers and bus bars is determined by tradeoffs between electrical resistance, emitter sheet resistance as well as technological restrictions in metal deposition process. An industry-standard $155 \times 155 \text{ mm}^2$ solar cell with screen printed front side grid has a finger width of $150 \mu\text{m}$ and two bus bars with a width of 2 mm [1]. Depending on the design of the photovoltaic module, up to approximately 10% of the entire silicon area can be covered by the metal resulting in shading loss. The metallic surface of the grid fingers and the bus bars reflects a larger part of the incoming light (over 90%). Therefore this portion of light does not contribute to the generated photocurrent. Only a small fraction of light is reflected at such angles that internal reflection at the front surface of the solar cell occurs potentially directing light to the silicon surface.

Different techniques can be adopted to reduce the shadowing effects of the metallic contacts. Besides extensive efforts to optimize the gridline arrangement [2] and the design of solar concentrators [3], local scattering structures induced either by microstructuring of the solar cell glass surface, or by using diffuse reflecting layers have been adopted for diverting light away from the contacts [4, 5]. The disadvantage of surface scatterers however is their sensitivity to environmental contaminations gradually leading to the reduced efficiency of the photovoltaic module.

In this work we introduce for the first time the advantages of using volumetric diffractive optical elements (DOE) based on local refractive index changes generated in the bulk of the cover glass. DOEs such as Fresnel zone plates and gratings are important components in manufacturing compact and multifunctional integrated optical devices such as micro-sensors, communication systems, and optoelectronic devices [6, 7]. They serve as planar and compact alternatives to refractive optics. Femtosecond laser-written single/multi layer gratings are generated in low iron content borosilicate glass with multi-hundred kHz pulses. The light diffraction resulting from these gratings is investigated experimentally and numerically as a function of grating parameters using the rigorous coupled wave analysis (RCWA) algorithm [9]. The resulting intensity distribution is investigated through far field images.

2. Design and numerical simulation approach

The purpose of the light management approach based on the use of a diffractive optical element e.g. volumetric grating is to reduce the portion of sunlight hitting the metalized areas such as grid fingers and busbars, and to divert the sunlight to non-metalized areas (Fig. 1, left).

The active part of a c-Si solar cell is located in the semiconductor layers, where the electron current is created. In order to collect the charge from the semiconductor and transfer it to the external load, a metallic grid and a back contact layer are deposited on the front and back semiconductor surfaces, respectively. The cell is laminated between two layers of an encapsulating

polymer (typically ethylene vinyl acetate, EVA) and attached to a backsheet for insulation and mechanical protection. The low-reflection cover glass serves for protection of the solar cell.

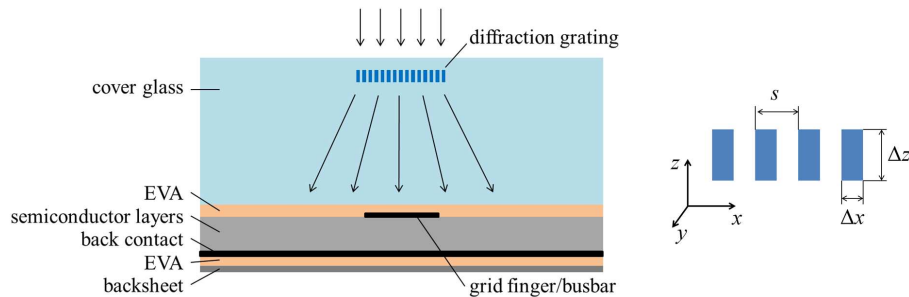


Fig. 1. Schematic principle of light diverting technique by introducing a volumetric diffraction grating in the bulk of the cover glass (left). Definition of the diffraction grating parameters (right).

By applying tightly focused femtosecond laser radiation permanent refractive index modifications can be generated in the cover glass locally without damaging the surrounding material. Depending on the radiation dose and material properties, refractive index changes on the order of $\Delta n = 10^{-2}$ have been reported [8]. In general this direct-writing technique can be applied to inscribe arbitrary three dimensional index modification patterns in the cover glass of the solar cell. However, to demonstrate the feasibility of the DOEs in this work we limit ourselves to the study of simple planar phase gratings. These gratings periodically modulate the phase of the incident light, which subsequently leads to an interference pattern at the boundary between cover glass and EVA/semiconductor layer. The grating parameters can be adapted in the way to maximize the amount of radiation diverted away from all metalized areas such as grid fingers and busbars. Parameters that can be varied include grating period s , number of lines N , as well as their position in the glass (Fig. 1, right). The achievable refractive index change Δn_{max} depends on irradiation parameters such as laser repetition rate, pulse energy, translation speed and focusing conditions.

To find a suitable set of DOE parameters and to obtain a quantitative estimation of the expected efficiency enhancement we performed RCWA calculations. For that, the solar cell was implemented as a 2D structure, which is divided into separated layers along the z -axis corresponding to the different materials (Fig. 1). Moreover, the system under consideration is invariant with respect to the y -direction, and periodic boundary conditions in the x -direction were assumed. The DOE is simplified as an ideal binary grating. Treating such multilayered periodic structures, the RCWA is a well-suited and very efficient numerical method taking reflections of light from metallic contacts, semiconductor layer and glass surfaces into account. It rigorously solves Maxwell's equations while dividing both the structure and the electromagnetic field into its Fourier components along the transverse direction. Consequently the numerical effort most strongly depends on the transverse feature sizes in our case mainly determined by the grating. On the other hand the large homogeneous regions (i.e. between the grating and the EVA/semiconductor layer) do not significantly increase the computational effort, in contrast to other common methods such as FDTD-simulations. Within these approaches the numerical effort largely scales with the size of the structure.

In the numerical model we considered normal incident light in a spectral range $\lambda=400$ -800 nm. The overall cell width was set to $x_c=2$ mm and the width of the metal contact was set to $x_m=200 \mu\text{m}$ to simulate the extreme case when about 10% of the entire cell area is covered by metalization. The grating was located $z=150 \mu\text{m}$ below the glass surface. We used the con-

stant refractive index values $n_{glass} = 1.51$ and $n_{silicon} = 4.2$ for the non-processed glass and the semiconductor respectively. The wavelength-dependent Drude model was adopted to calculate the reflection from the metal contacts. The effect of the EVA on the calculation results was neglected to simplify the analysis.

3. Ultrafast laser-induced refractive index changes

In the first step, the process parameter windows for crack-free modifications featuring maximum index change Δn_{max} were investigated to provide input for the numerical simulations. Laser radiation produced by the FCPA laser system IMRA μ Jewel 400D ($\lambda=1043$ nm, $f_{rep}=0.1-5$ MHz, $t_p \simeq 500$ fs) and focused with a $20\times/N.A.=0.4$ microscope objective into the cover glass (low iron borosilicate glass) with the thickness $d = 2.87$ mm was used to generate permanent refractive index changes. The glass samples can be translated by a computer controlled 3D stage (Aerotech, ALS130). The experimental setup for the material irradiation is described in more details elsewhere [10]. Material processing parameters such as the laser pulse energy, the repetition rate and the translation velocity were varied to obtain modification tracks while moving the sample continuously along the y axis. The refractive index modifications were induced at a constant distance $z=150$ μ m from the upper glass surface. Cross-sections of the tracks produced (Fig. 2 a) were prepared by lapping and polishing to investigate the dimensions of the structures obtained and to ensure that they are free of cracks.

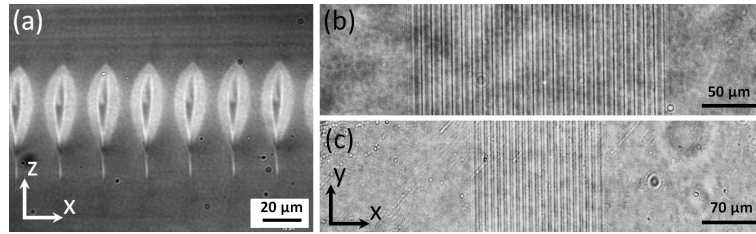


Fig. 2. Femtosecond laser written modification in the cover glass of a solar cell: (a) cross section, (b) grating with 25 lines, (c) grating with 20 lines.

In the second step periodic gratings with the grating periods equal to the doubled measured structure width, $s = 2\Delta x$, were produced (Fig. 2 b, c). In order to determine the amount of the induced refractive index change, the gratings were illuminated by a green HeNe laser at 543 nm and the intensities of the occurring diffraction orders were measured. Subsequently a numerical evaluation method based on an iterative Fourier transform algorithm [11] was applied. This algorithm was capable of retrieving the phase information $\Delta\phi(x)$ of the investigated gratings from the measured intensity pattern. Finally, the corresponding refractive index was extracted by combining the phase with the height distribution $h(x)$ of the grating lines (Fig. 2 a) by eq. 1.

$$\Delta\phi(x) = \frac{2\pi}{\lambda} \int_0^{h(x)} \Delta n(x, z) dz. \quad (1)$$

After evaluation of the produced data the processing parameters resulting in modification tracks with the largest Δn at the largest translation speed v were chosen for the numerical simulations. The resulting peak refractive index change $\Delta n_{max}=1.06 \times 10^{-3}$ was obtained at the repetition rate $f_{rep}=200$ kHz, the pulse energy $E_p=1.75$ μ J and the translation speed $v=10$ mm/s. The resulting tracks width was $\Delta x=10$ μ m, and the track height was $\Delta z=46$ μ m.

4. Study of the efficiency enhancement

To study the efficiency enhancement induced by the grating, the processing parameters obtained in Sec. 3 were taken to be fixed values, whereas both the number of lines N in the grating and the grating period s were varied. Moreover, multiple grating layers placed on top of each other (stacks) were taken into consideration.

To compare all calculations and to estimate the resulting efficiency change of the photovoltaic module, the figure of merit was chosen to be the number of photons transmitted into the semiconductor layer. It can be obtained by weighting the transmitted intensity with the number of photons provided by the solar spectrum and subsequently integrating over the whole spectral range of interest. To quantify the efficiency enhancement factor, this number was then compared to the number of photons transmitted through a structure without a diffraction grating.

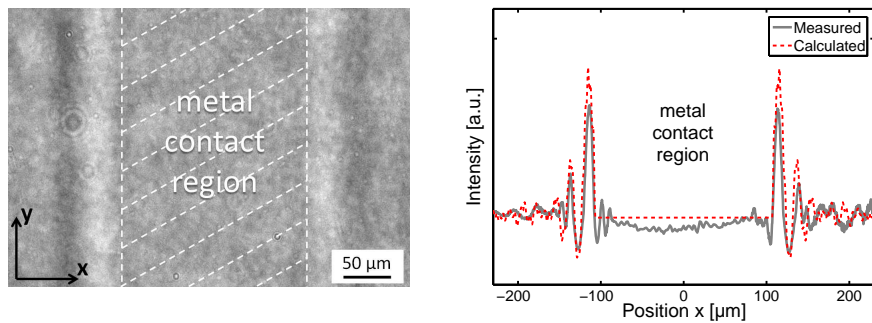


Fig. 3. Farfield image of the intensity distribution produced by a grating with $s = 20 \mu\text{m}$, $\Delta x = 10 \mu\text{m}$ (left). Comparison of the measured averaged intensity distribution with the calculated data (right).

To test the efficacy of this new light-diverting technique, a test grating ($s = 20 \mu\text{m}$, $\Delta x = 10 \mu\text{m}$) was first produced. The resulting intensity distribution at the virtual interface between the glass and semiconductor was measured using a CCD device and a white light source with an emission spectrum close to that of natural sun light (Fig. 3). The measured efficiency enhancement of the intensity effectively reaching the silicon substrate for this parameter set was rather weak (less than 0.3%) in this first test, but was in good agreement with the calculated data. As a consequence these results justified further optimization of the grating parameters and the laser processing parameters.

Based on the results obtained for a single layer grating a systematic study of the efficiency enhancement was then performed by varying the number of layers, the number of lines in a grating, and the grating period. In order to compare the results, for each set of the parameters selected, RCWA calculations were performed using $\Delta x = 9 \mu\text{m}$ as a fixed value for the line width. In Fig. 4(a) the influence of the number of layers on the efficiency enhancement is shown for up to 10 layers stacked on top of each other with the uppermost layer still located $z=150 \mu\text{m}$ below the glass surface. The maximum increase in efficiency about 2.8% was achieved for a grating consisting of 8 layers. Further increase of the layers number resulted in gradual efficiency decrease. The intensity distribution and the corresponding efficiency increase is shown in Fig. 4(b) for gratings with 1 and 8 layers.

To study the dependency of the efficiency enhancement on the number of lines in the grating and the grating period, calculations were made for both the cases of 1 and 8 stacked layers

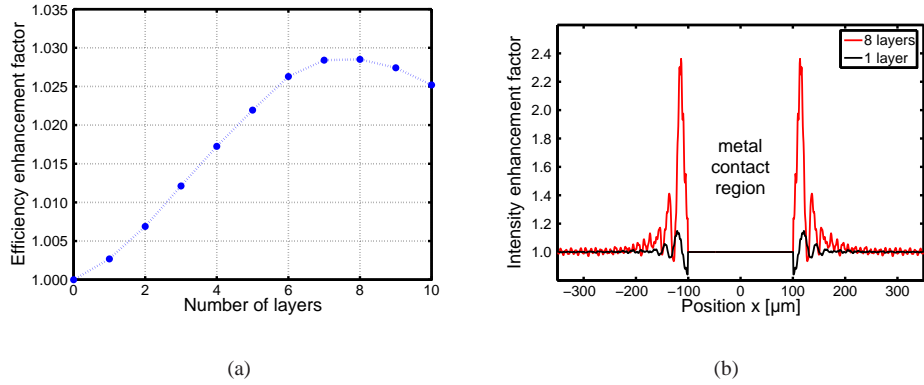


Fig. 4. (a) Calculated dependency of the efficiency enhancement factor on the number of layers. (b) Calculated intensity enhancement distribution for 1 and 8 layers in a grating with $N = 9$, $\Delta x = 9 \mu m$ and $s = 18 \mu m$.

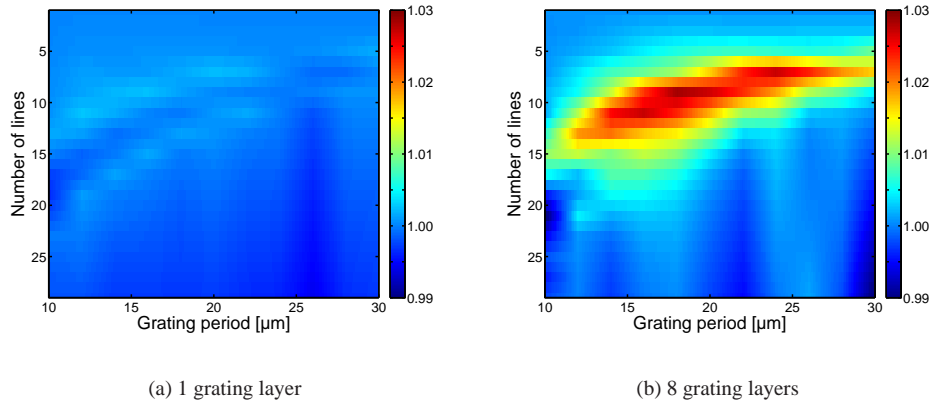


Fig. 5. Calculated dependency of the efficiency enhancement factor on the number of lines N and the grating period s for different number of grating layers.

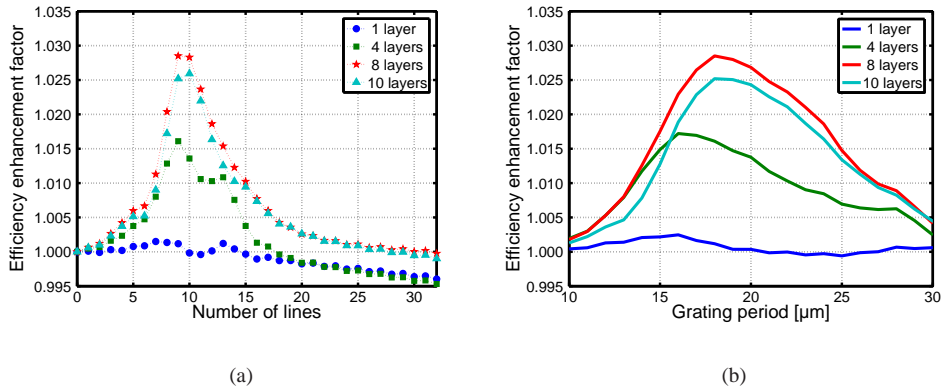


Fig. 6. Calculated efficiency enhancement factor for different number of grating layers: (a) Dependency on the number of lines for a constant grating period $s = 18 \mu\text{m}$, (b) dependency on the grating period at a constant number of lines $N = 9$.

(Fig. 5). The maximum increase in efficiency was found for $N = 9$ lines and the grating period $s = 18 \mu\text{m}$ which corresponds to a grating with a duty cycle of 0.5 and covers the entire area of the metal contact. Too many lines would start to cover the parts of the light-absorbing semiconductor area and therefore reduce the efficiency due to extensive backscattering of the incident light. Selecting grating periods significantly larger than $s = 2\Delta x$ would also reduce the diffraction efficiency of the grating. The dependency of the efficiency increase factor on the number of lines and the grating period is shown in Fig. 6 for 1, 4, 8 and 10 grating layers.

In our calculations normal incident light was assumed to simplify the efficiency enhancement analysis. However a slight deviation from normal incidence could cause a significant change of the optical function resulting in decreasing efficiency. To estimate this effect, calculations were performed for the incidence angle deviation of $\alpha=10^\circ$. For a grating with the same geometrical parameters the efficiency increase was only about 1% compared to 2.8% for the normal incidence case.

The approach we present here can be extended to planar and volumetric DOEs such as Fresnel lenses and their combinations. The efficiency of the light diverting can be further increased by optimization of process parameters for refractive index modification in glass. While this study represents the first proof of concept, the processing time for the entire $155 \times 155 \text{ mm}^2$ solar cell module would be approximately 2 hours for microstructuring at 8 depth levels and the translation speed $v=10 \text{ mm/s}$ as adopted in our experiments. Assuming energy scalability of the laser processing and utilizing kW-power level ultrafast lasers [12] and parallel/multi-focus processing, the overall processing speed can be greatly increased. Potentially a productivity increase by a factor of about 3000 can be achieved which would reduce the processing time to several seconds per photovoltaic module.

5. Conclusion

Volumetric diffractive optical elements such as simple diffraction gratings produced by a direct laser writing technique using ultrafast laser radiation can be adopted for effective light management in photovoltaic modules. Shadowing effects caused by the metalization can be significantly reduced by deflecting light away from metal contacts such as grid fingers and busbars. Diffraction gratings were produced in low-iron-containing borosilicate glass by changing

its refractive index locally on the micrometer scale. Appropriate laser processing parameters were found for a crack-free modification of bulk glass with permanent refractive index change of $\Delta n_{max}=1.06 \times 10^{-3}$. Test gratings produced in glass demonstrate the feasibility of this light management technique, with resulting intensity distribution being in a good agreement with calculations based on the RCWA approach. Further numerical investigations towards efficiency enhancement prove that depending on the parameters of the grating, such as the number of layers, the grating period and the cell geometry e.g. the area portion covered by metalization, efficiency increase of about 2.8% can be achieved.

6. Acknowledgments

This work was supported by the Fraunhofer-Townes Collaboration between the Townes Laser Institute and the Fraunhofer Institute for Laser Technology. We would also like to thank A. Stephanides from the RWTH Aachen University for his help performing irradiation experiments and sample characterization.